Biochimica et Biophysica Acta 898 (1987) 202–213
Elsevier

BBA 73514

Estimation of spin probe clustering in biological membranes

Larry M. Gordon [a], Frank D. Looney [b] and Cyril C. Curtain [b]

[a] *Rees-Stealy Research Foundation, San Diego, CA (U.S.A.) and* [b] *Biotechnology Section, Division of Chemical and Wood Technology, CSIRO, Clayton, Vic. 3168 (Australia)*

(Received 30 June 1986)
(Revised manuscript received 10 December 1986)

Key words: Erythrocyte membrane; Radical interaction; Fluidity; Probe clustering; Spin probe; ESR; (Human erythrocyte ghost)

An iterative spectral subtraction technique has been developed which accurately estimates the proportion of 'dilute' and 'clustered' I(12, 3) (i.e., 5-nitroxide stearate) in human erythrocyte ghosts at 37°C, even if subtractant spectra free from probe–probe interactions cannot be measured due to technical limitations. Gordon et al. ((1985) J. Membrane Biol. 84, 81–95) earlier showed that I(12, 3) occupies a class of high-affinity sites in ghosts at probe/total lipid ratios (P/L) less than 1/2250. Saturation occurs with increasing probe concentration, and, at higher loading, the probe inserts itself at initially dilute sites to form membrane-bound clusters of variable size. Although this model allows determination of the dilute/clustered probe ratio, it requires subtraction of experimental spectra with a 'magnetically dilute' spectrum obtained using $P/L < 1/4600$. The new methodology accurately profiles the % probe clustering in human erythrocyte ghosts over the entire P/L range, even if the lowest P/L for the subtractant spectrum contains substantial probe–probe interactions (i.e., P/L of 1/604 or 1/303). Application of either the subtraction technique in Gordon et al. (1985) or the iterative subtraction protocol described here should allow determination of probe clustering in a wide range of I(12,3)-labeled biological membranes.

Introduction

In a classic ESR study of sarcoplasmic reticulum at 37°C, Scandella et al. [1] demonstrated that a spin-labeled phospholipid migrates rapidly in the plane of the lipid bilayer with a lateral diffusion coefficient (L_D) of $6 \cdot 10^{-8}$ cm^2/s. By assuming that the phospholipid spin probe partitions ideally into the membrane, diffusion rates were calculated from the spectral broadening due to the spin-exchange that occurs between colliding probe molecules.

Despite the success of the above diffusion model in interpreting the broadened ESR spectra of spin-labeled phospholipids in sarcoplasmic reticulum, it is not applicable for other membranes labeled with spin probes that do not resemble endogenous components. One example of an 'unphysiologic' label is the fatty acid derivative, I(12, 3). This probe has been widely used since it readily incorporates into a variety of model [2] and biological [3] membranes. However, in a recent investigation of human erythrocyte ghosts labeled with I(12,3) at 37°C, spectral alterations occurring with increased probe/total lipid ratios (P/L) were not principally due to the spin-ex-

Abbreviations: ESR, electron spin resonance; I(12, 3), the *N*-oxyl-4′,4′-dimethyloxazolidine derivative of 5′-ketostearic acid; P/L, the ratio of probe molecules to total lipid molecules; L_D, lateral diffusion coefficient (cm^2/s).

Correspondence: L.M. Gordon, Rees-Stealy Research Foundation, 2001 4th Avenue, San Diego, CA 92101, U.S.A.

change between probe molecules which collide when executing rapid lateral diffusion [4]. Instead, a model was developed for I(12, 3) distribution in which the spin probe occupies a class of high-affinity, non-interacting sites at low loading. Saturation occurs when the probe concentration is increased, and, at higher loading, the probe inserts itself at initially dilute sites to form membrane-bound clusters of variable size. No 'low' probe remains at higher P/L where all I(12, 3) clusters in a 'concentrated' phase. Assuming that the exchange-rate between 'clustered' and 'low' states is slow on the ESR time-scale (10^{-8} s), subtractions of 'low' spectra * from intermediate-range spectra were performed to artificially simulate the alterations seen upon probe addition, and to assess relative proportions of concentrated and dilute probe from double integrations of component spectra. Thus, I(12, 3) interactions in erythrocyte ghosts are not consistent with the diffusion model but instead resemble the phase separation of enriched phospholipid spin probe observed in sarcoplasmic reticulum below 20°C [1].

However, the above protocol for determining probe clustering is subject to technical limitations. A P/L of 1/4600 was confirmed as being 'magnetically-dilute' in I(12, 3)-labeled human erythrocyte ghosts only when subtraction of a spectrum at a P/L of 1/16000 from that of 1/4600 gave background noise. For membranes labeled with such extremely low P/L, obtaining suitable spectra requires an ESR spectrometer with high sensitivity, elevated membrane concentrations (> 50 mg lipid/ml), and/or signal-averaging over extended times (about 1 h). In practice, these conditions may be difficult to meet. Since a given membrane (e.g., plasma membrane) must frequently be prepared so that it is free of contaminating organelles (e.g., endoplasmic reticulum, mitochondria), high yields of pure membranes are the exception. Moreover, whole cells are often used in spin-label experiments, and, in such instances, membrane concentrations can be raised only to that level found with packed cells. Lastly, signal-averaging experiments are not reliable for assigning 'magnetically-dilute' spectra if the ESR signal changes with time.

In this paper, a method is developed to estimate probe clustering in human erythrocyte ghosts at 37°C that does not require isolation of the 'magnetically-dilute' spectrum ($P/L \leq 1/4600$). It is based on the previous finding that: (i) 'magnetically-dilute' probe occurs to varying degrees in the intermediate range; and (ii) the 'clustered' component is not unique for each probe concentration in the intermediate range, but consists of variable-size clusters that are shared to some extent in the various 'concentrated' states [4]. Hence, an 'intermediate-range' spectrum of I(12, 3)-labeled erythrocyte ghosts at a P/L of 1/604 may be incrementally subtracted from a spectrum at higher P/L (e.g., 1/303 or 1/101) to yield the spectral alterations seen experimentally on raising the probe concentration. If the non-magnetically-dilute P/L of 1/604 is used as the subtractant spectrum rather than that of the 'magnetically-dilute' P/L of 1/4600, then double integration of the residual spectrum obtained at the subtraction endpoint yields an 'apparent' clustering which underestimates the actual clustering. Nevertheless, accurate estimates of the true probe clustering may be obtained by using, as subtractant species, spectra of membranes labeled with P/L ranging from 1/604 to that of the experimental spectrum to be subtracted. Plots of the % ('apparent' clustering for the given P/L) vs. the probe concentration of the subtractant spectra may then be constructed, and extrapolation of the probe concentration of the subtractant spectrum to 'zero' produces probe clustering agreeing with that determined using the P/L of 1/4600 spectrum as the subtractant species.

Materials and Methods

I(12, 3) was obtained from Syva Co., Palo Alto, CA, and thin-layer chromatographic analysis demonstrated negligible impurities. All other reagents were obtained from Sigma Chemical Co., St. Louis, MO.

Human erythrocyte ghosts were obtained according to Dodge et al. [5] and suspended in 100 mM tris (pH 7.4) at 5 mg protein/ml. Samples

* For human erythrocyte ghosts at 37°C, the 'low', or 'magnetically-dilute', P/L range is $< 1/2250$, the 'intermediate' P/L range is 1/2250 to 1/24, and the 'very-high' P/L range is $> 1/24$ [4].

were used after storage at −20 °C. Protein was determined by the method of Hartree [6]. Ghosts were assumed to be 50% protein and 50% lipid on a weight basis.

Spin-labeling of ghosts was performed as described earlier [4]. The extent of I(12, 3) incorporation was tested by comparing the amount of probe added to the ghost suspension (i.e., μg I(12, 3)/mg protein 'wt') with the paramagnetic spins observed in the microwave cavity (i.e., μg I(12, 3)/mg protein 'spins'). The number of spins was calculated from the ratio of the double-integrated spectrum of I(12, 3)-labeled ghosts with that of the Varian strong-pitch reference (0.1% pitch, with $3 \cdot 10^{15}$ spins in 5.5 mm [1,4]). The spin label/membrane ratios for the probe in the cavity were 0.80 to 45 μg I(12,3)/mg erythrocyte protein (or 1 probe per 604 to 9 lipid). The P/L was calculated assuming all lipid to be phospholipid and cholesterol [5].

ESR spectra of I(12, 3)-labeled erythrocyte ghosts (Fig. 1) were recorded with a Varian E-104A spectrometer equipped with a temperature regulator. Pipettes containing the sample were placed in a special holder (attributed by Gaffney to R. Kornberg [7] and fabricated out of Kel-F by John Markel (J & M Specialities, San Diego, CA)) which was mounted in the temperature accessory. This holder facilitates reproducible positioning of the capillary pipette, and is critical for performing accurate spectral subtractions. The spectra were digitized into 1470 points with a Hewlett-Packard 7470A plotter and 9816 computer. Additions, subtractions and integrations were performed on stored data. Computer programs written in Hewlett-Packard's HPL language are available from the authors on request.

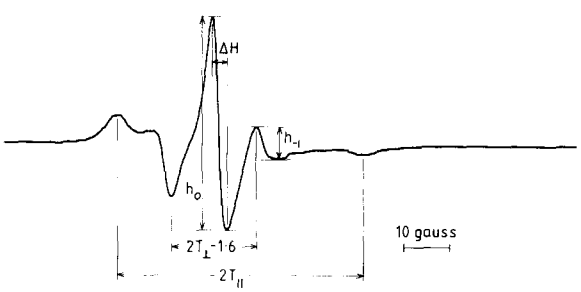

Fig. 1. ESR spectrum of I(12, 3)-labeled human erythrocyte ghosts at 37 °C, recorded with an 8 min scan time, 5000 receiver gain, 2 gauss modulation amplitude, 10 mW microwave power, and 1 s time-constant. Outer and inner hyperfine splittings, $2T_{\parallel}$ and $2T_{\perp}$, were measured as shown; $2T_{\perp}$ was corrected by the addition of 1.6 gauss [2]. The peak-to-peak distance of the central line (ΔH) is indicated. Respective heights of the central line (h_o) and the high-field peak of the inner hyperfine doublet (h_{-1}) are shown. The μg probe/mg protein and P/L ratios, determined from the number of spins in the spectrum, were 0.80 and 1/604, respectively (see Materials and Methods and Scandella et al. [1]). The horizontal bar indicates 10 gauss.

Probe-probe interactions have also been estimated using three empirical parameters [3,8,9]. The first involves measuring the peak-to-peak width of the central line (i.e., ΔH of Fig. 1).

$$\Delta H = \Delta H_o + \Delta H_{dip} + \Delta H_{ex} \quad (1)$$

where ΔH_o is the linewidth without interactions, ΔH_{dip} is the line broadening caused by magnetic dipolar interaction, and ΔH_{ex} is contributed by spin-spin exchange [3]. Enhanced probe–probe interactions increase ΔH.

The second measure is based on the observation that $T_{\perp}$, but not $T_{\parallel}$, broadens with increasing P/L in various membranes, including erythrocyte ghosts [3,9,10]. Thus, with $\Delta T_{\parallel}$ remaining zero, positive increases in $T_{\perp}(\Delta T_{\perp})$ indicate greater probe–probe interactions.

The third parameter depends on the height of the high-field peak of the inner hyperfine doublet (h_{-1} in Fig. 1) decreasing with respect to that of the central line (h_o): h_{-1}/h_o declines as the probe concentration is elevated [3,8].

Results and Discussion

Spin-labeling of human erythrocyte ghosts

I(12, 3) incorporation was tested by comparing the weight of the probe added to membranes (Fig. 2) with that calculated from the spins in the spectrum. For μg probe/mg protein 'wt' ratios of 2 to 500, erythrocyte ghosts show only a limited capacity for I(12, 3), uptake. Progressively decreased incorporation occurred at higher loading. These results are consistent with earlier probe titrations which indicated that I(12, 3) binds to the ghosts at specific membrane sites [4]. For low levels of bound probe, I(12, 3) apparently binds to a single class of high-affinity sites. However, the I(12, 3)-binding isotherm exhibits such significant

curvature at high loading (see Fig. 2B of Ref. 4) that the probe uptake is reduced. Although one explanation for this behavior is that I(12, 3) binds to two classes of independent sites, it is more likely that the probe-membrane sites, when occupied at high loading, act through a cooperative mechanism to inhibit further I(12, 3) binding (see below and ref. 4).

One cautionary note should be raised concerning the above measurement of spin-probe concentrations. To the extent that the dielectric loss and lens effect, and also the filling factor, of the membrane sample differ from those of the Strong-Pitch, uncertainty will be introduced into the measurement of the absolute number of spins. However, all comparisons are here made between erythrocyte ghosts labeled with varying amounts of probe (Fig. 2). The critical point is whether the instrument responds linearly over a wide range of spins. This was tested by preparing a concentrated stock solution of I(12,3) in 100% ethanol, and using it to make dilute probe aliquots to match those concentrations in Fig. 2. The number of spins, determined from double-integration of the spectra of I(12, 3) in ethanol and Strong-Pitch, increased linearly with increasing amounts of I(12,3) in ethanol. On the other hand, the corresponding plot for I(12, 3)-labeled erythrocyte ghosts plateaued at high probe loading, confirming reduced probe uptake with increasing probe concentrations (data not shown).

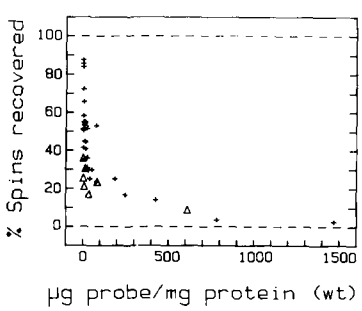

Fig. 2. Plot of % recovered spins vs. weight of probe added to 60 μl membrane aliquots. % Recovered spins were calculated from the ratio of the probe weight added to the sample (i.e., μg probe/mg protein 'wt') to that determined from the spins in the spectra (i.e., μg probe/mg protein 'spins'). Ghosts were suspended at 12, 42 or 83 mg protein/ml (+) (data adapted from Ref. 4) or 5 mg protein/ml (△) (this report).

The reduced I(12, 3) uptake at high loading is due to the erythrocyte ghosts having a limited capacity for binding probe. Excess probe remains on the side of the microfuge tube as a waxy deposit [4]. This was verified by adding ethanol to the tube containing I(12, 3)-labeled membranes at 50% (v/v). Such treatment completely solubilizes both probe and membrane, leaving only an isotropic spectral component indicating I(12,3) freely tumbling in solution. If a dilution correction is included, double integration of these spectra shows 100% recovery of I(12,3) spins for each μg probe/mg protein 'wt' ratio in Fig. 2.

To test whether the Strong-Pitch calibration yields an accurate absolute number of spins, a I(12, 3) preparation was examined that was found to be greater than 95% pure on thin-layer chromatography [3]. Using the double-integration technique, the number of spins determined for I(12, 3) in ethanol (25 mg probe/ 2 ml ethanol) was within experimental error to that calculated assuming all probe molecules to have an unpaired electron. This suggests that discrepancies between dielectric constants and sample geometries do not introduce significant error into calculation of absolute spins.

Since μg probe/mg protein 'wt' does not accurately indicate probe insertion, all P/L (or μg probe/mg protein) ratios used in the following experiments were assessed from the paramagnetic spins of the spectrum.

Effects of I(12, 3) concentration on spectra of human erythrocyte ghosts

The ESR spectra of I(12, 3)-labeled erythrocyte ghosts were recorded with P/L ranging from 1/604 to 1/9 (Fig. 3). At a P/L of 1/604, the spectrum indicates that the probe undergoes rapid anisotropic motion about its long molecular axis at 37 °C (Fig. 3a). Raising the P/L from 1/604 to 1/24 decreased h_{-1} with respect to h_o, displaced downward the high-field baseline and upward the low-field baseline, increased $2T_\perp$ and ΔH and left $2T_\parallel$ unchanged (Fig. 3b–f). Further increasing the P/L above 1/24 achieved a 'very-high' range, denoted by noticeably broadened spectra and sloping baseline (Fig. 3g). Hyperfine splittings and ΔH could not be measured at this high loading. In the 'very-high' range, liquid-lines were present

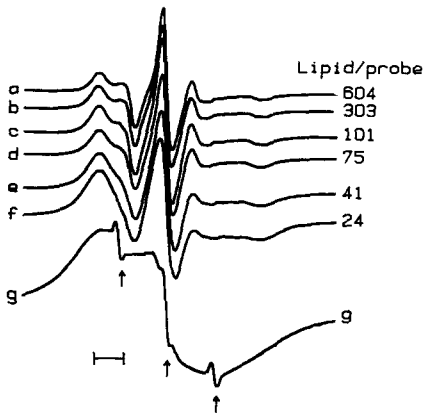

Fig. 3. ESR spectra of human erythrocyte ghosts (5 mg protein/ml at 37°C) labeled with varying concentrations of I(12, 3). Lipid/probe (μg probe/mg protein) ratios were: (a) 604 (0.80); (b) 303 (1.59); (c) 101 (4.77); (d) 75 (6.44); (e) 41 (11.67); (f) 24 (20); (g) 9 (45). The liquid lines indicated by arrows in Fig. 3g are due to I(12, 3) tumbling rapidly in aqueous solution. The horizontal bar indicates 10 gauss.

due to the probe tumbling rapidly in the aqueous solution.

Similar probe-dependent spectral alterations have been reported both with I(12, 3)-labeled intact erythrocytes [11], and erythrocyte ghosts [10,12]. For reasons described in detail elsewhere [3,4,8–10], these perturbations are probably not due to probe-dependent fluidizations of the membrane, but rather are the result of enhanced ΔH_{ex} arising from I(12, 3) interactions. Although no single spectral feature for ghosts labeled with a P/L of 1/604 is characteristic of exchange-broadening, comparison of Fig. 3a with spectra of human erythrocyte membranes labeled with a P/L of 1/16000, 1/4600 or 1/2250 (Fig. 3ab of Ref. 4) indicates significant radical interactions.

Physical models of membrane-probe distribution

It is important to establish the physical basis for probe–probe interactions. One possibility is that I(12,3) partitions uniformly into bulk-membrane lipid, and the spectral broadening is principally due to spin exchange between probe molecules which transiently collide when executing rapid lateral diffusion. Although this diffusion model may be appropriate for analyzing phospholipid spin probes incorporated into model and biological membranes [1], it is completely inadequate for the I(12, 3)-erythrocyte ghost system for several reasons. First, the Scandella et al. [1] model implicitly requires that the I(12, 3) probe partitions into red cell membranes as an infinitely-dilute solute in an ideal solvent. However, Fig. 2 shows that probe uptake by the membrane is substantially reduced at those P/L where spectral broadening occurs. Thus, probe uptake cannot here be interpreted in terms of a partitioning phenomenon. Instead, it must reflect: (i) I(12, 3) binding to two classes of independent sites (i.e., 'low'- and 'high'-affinity sites) and/or (ii) cooperative binding, such that I(12, 3) uptake is reduced at high probe loading (see Ref. 4). Since the decreased probe uptake occurs at the same P/L where spectral broadening occurs, an important initial condition for legitimately mixing in spin-spin exchange via modified Bloch equations [13] has been invalidated. Second, following the Scandella et al. [1] model, a L_D of $3 \cdot 10^{-7}$ cm^2/s may be calculated from the ΔH broadening (Fig. 4A of Ref. 4). Thus, the Scandella et al. [1] model provides a physically impossible description of I(12, 3) distribution and dynamics in erythrocyte ghosts. The above L_D would rank erythrocytes as one of the most fluid biological membranes ever examined. Yet, this picture disagrees with the finding that the I(12, 3)-labeled erythrocyte is one of the least fluid membranes, as assessed by order parameters sensitive to probe flexibility. Also, it is well known that penetrant proteins and incorporated fluorescent probes each have low L_D in the erythrocyte membrane [4].

In an earlier study, Gordon et al. [4] developed an alternative, cluster model to show that the broadened spectra of I(12, 3)-labeled erythrocyte ghosts reflect: (i) an anisotropic spectrum due to the magnetically-dilute probe molecules occupying membranes sites; and (ii) 'concentrated' spectra that do not necessary reflect a unique species, but instead represent variable-sized clusters in the membrane. This model presumes that the probe-exchange between 'dilute' and 'concentrated' states is slow on an ESR time-scale (10^{-8} s), but makes no implicit assumption about the nature of the 'concentrated' spectrum. In Gordon et al. [4], the above model was tested by subtracting incremental amounts of a low-range spectrum ($P/L =$

1/4600) from intermediate-range spectra with P/L ranging from 1/2250 to 1/38. After establishing the subtraction endpoint, relative proportions of 'dilute' and 'concentrated' probe were assessed by double integration of component spectra. The principal legitimacy of subtracting low-range spectra from intermediate-range spectra rests on the accurate simulation of spectral features observed experimentally at higher loading. When such subtractions are performed, the key parameters (i.e., $2T_{\parallel}$, $2T_{\perp}$, ΔH, h_{-1}/h_o) each change in the direction seen experimentally with increasing probe concentration (Figs. 10, 11 of Ref. 4).

Using the above cluster model, Gordon et al. [4] showed that intermediate-range spectra of ghosts (P/L of 1/604 to 1/24) were composites reflecting 'dilute' probe and membrane-bound clustered (or 'concentrated') probe [4]. Only at low P/L ($< 1/2250$) does I(12, 3) bind to high-affinity sites to yield 'magnetically-dilute' spectra. Saturation occurs with increasing P/L and, at a higher loading (P/L of 1/604 to 1/24), occupied sites act as nuclei for inserting additional probe. The affinity of occupied sites for additional I(12, 3) is much less than that of unoccupied sites at low P/L.

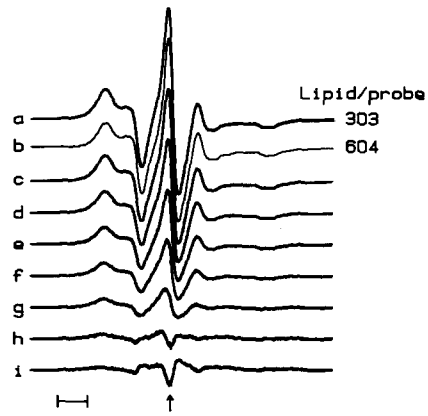

Fig. 4. Subtraction spectra, obtained by subtracting increasing amounts of an intermediate-range spectrum (b) at a $P/L = 1/604$ from another intermediate-range spectrum (a) at a higher loading of $P/L = 1/303$; h_o of (b) is normalized to that of (a). (c), (d), (e) and (f) are residual spectra, with double-integrated intensities of 84%, 68%, 53% and 37% of that of the unsubtracted $P/L = 1/303$ spectrum. (g) This is the spectral endpoint of the subtraction (i.e., 'apparent concentrated' spectrum) as defined in the text. 'Apparent dilute' and 'apparent concentrated' probe are 79 and 21; and were determined from double integration of the (a) and (g) spectra. (h) and (i) are residual spectra, with double-integrated intensities of 5.2% and 0.3% of that of the unsubtracted $P/L = 1/303$ spectrum. These are over subtracted, as indicated by the descent of the mid-field peak (see arrow). The horizontal bar indicates 10 gauss.

Estimation of I(12, 3) clustering in human erythrocyte ghosts

The analysis of Gordon et al. [4] is modified here to consider if probe clustering may be estimated using, as the subtractant species, the intermediate-range spectra (e.g., $P/L = 1/604$) where some of the probe interactions are manifest. This approach is based on the subtractant spectrum at a P/L of 1/604 being primarily due to 'dilute' probe [4] and having a probe distribution shared to some extent by membranes at higher P/L. Subtraction with the 1/604 spectrum may provide an estimate of the actual probe clustering for membranes labeled with more probe. Accordingly, incremental amounts of the 1/604 spectrum (Fig. 4b) were subtracted from a higher P/L (1/303) spectrum (Fig. 4a). Fig. 4c–g shows that the 'subtracted' spectra accurately mimic those alterations observed when I(12, 3) is added to ghosts labeled with a P/L of 1/303 (Fig. 3c–f). That is, removing the P/L of 1/604 spectrum increased $2T_{\perp}$ and ΔH, decreased h_{-1}/h_o, but left $2T_{\parallel}$ unaffected. The subtraction endpoint was identified by the high-field peak of the central band falling below the baseline (see arrow in Fig. 4i). This is due to oversubtraction such that the 1/604 spectrum appears in inverse phase.

Despite some probe-probe interactions occurring in the P/L of 1/604 spectrum, the above results suggest that subtracting this spectrum from the one at a P/L of 1/303 is a legitimate operation, since the spectral changes seen at higher loading are appropriately simulated. It is of interest to consider the intermediate-range spectrum from which all P/L of 1/604 has been removed (Figs. 4g, 8a). This 'concentrated' spectrum shows anisotropic properties, such as a well-defined inner splitting, and also broadened characteristics due to radical interactions; the 'concentrated' probe is probably membrane-bound and clustered. Double integration of the component spectrum (Fig. 4g) indicates that the P/L of 1/303 spectrum consists of probe in the '1/604' state (79%)

and the 'concentrated' state (21%). However, the proportion of probe in the 1/604 state is more properly defined as 'apparent dilute', while that in the unsubtracted portion of the 1/303 spectrum (Figs. 4g, 8a) is 'apparent concentrated'. Because probe–probe interactions are present in the 1/604 spectrum, the 'apparent concentrated' (21%) and 'apparent dilute' (79%) states determined from the 1/303 spectrum (Fig. 4g) are underestimated and overestimated, respectively (see below). Clearly, there is considerable 1/604 spectral character residing in the 1/303 spectrum, consistent with our working hypothesis that a portion of the probe distribution at P/L of 1/604 is shared by the 1/303 state.

Applying this subtraction protocol to the intermediate-range spectra at higher loading (i.e., subtracting P/L of 1/604 from 1/101, 1/75 and 1/24) also generated spectral changes (Figs. 5–7) which are seen experimentally with increases in the probe/lipid (Fig. 3a–f). Here, however, endpoints were assigned by the central band first becoming asymmetric and then a shoulder arising on its high-field side (Figs. 5–7). Each of these effects was the result of oversubtraction such that the P/L of 1/604 spectrum appears in inverse phase. 'Apparent concentrated' spectra were determined as those immediately before central-band peak asymmetry and shoulder (Figs. 5f, 6f, 7d). In each instance, the 'concentrated' spectrum is characteristically broadened over the corresponding unsubtracted spectrum, with increased $2T_{\perp}$ and ΔH, decreased h_{-1}/h_o, and $2T_{\parallel}$ unchanged (Fig. 8b–d). It was not possible to remove any P/L of 1/604 spectrum from a 'very-high' range spectrum (e.g., Fig. 3g) without oversubtracting, and therefore suggests that there is no '1/604' character in the P/L of 1/9 spectrum.

The percentage of 'apparent' probe clustering, which was assessed from the residual spectrum

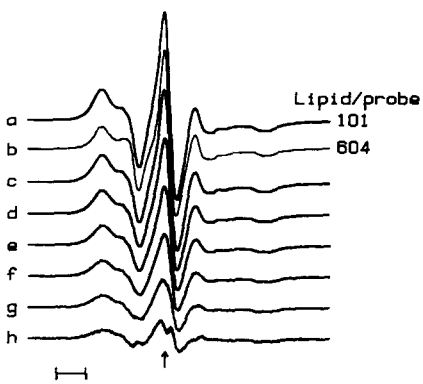

Fig. 5. Subtraction spectra, obtained by subtracting increasing amounts of an intermediate-range spectrum (b) at a $P/L = 1/604$ from another intermediate-range spectrum (a) at a higher loading of $P/L = 1/101$; h_o of (b) is normalized to that of (a). (c), (d) and (e) are residual spectra, with double-integrated intensities of 87%, 74%, and 60% of that of the unsubtracted $P/L = 1/101$ spectrum. (f) This is the endpoint of the subtraction (i.e., 'apparent concentrated' spectrum) as defined in the text. 'Apparent dilute' and 'apparent concentrated' probe are 46 and 54%, and were determined from double integration of the (a) and (f) spectra. (g) and (h) are residual spectra, with double-integrated intensities of 33% and 19% of that of the unsubtracted $P/L = 1/101$ spectrum. These are oversubtracted, as indicated by the asymmetry of the central band and appearance of a shoulder due to the subtractant spectrum in inverse phase (see arrow). The horizontal bar indicates 10 gauss.

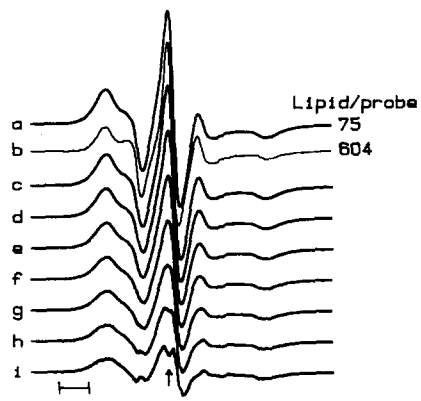

Fig. 6. Subtraction spectra, obtained by subtracting increasing amounts of an intermediate-range spectrum (b) at a $P/L = 1/604$ from another intermediate-range spectrum (a) at a higher loading of $P/L = 1/75$; h_o of (b) is normalized to that of (a). (c), (d) and (e) are residual spectra, with double-integrated intensities of 95%, 89% and 84% of that of the unsubtracted $P/L = 1/75$ spectrum. (f) This is the spectral endpoint of the subtraction (i.e., 'apparent concentrated' spectrum) as defined in the text. 'Apparent dilute' and 'apparent concentrated' probe are 22 and 78%, and were determined from double integration of the (a) and (f) spectra. (g), (h) and (i) are residual spectra, with double-integrated intensities of 73%, 67% and 62% of that of the unsubtracted $P/L = 1/75$ spectrum. These are oversubtracted, as indicated by the asymmetry of the central band and appearance of a shoulder due to the subtractant spectrum in inverse phase (see arrow). The horizontal bar indicates 10 gauss.

obtained by subtracting all 1/604 spectrum from the spectra recorded at higher loading, is plotted as a function of the probe concentration in Fig. 9. This plot is contrasted with that obtained earlier by using a 'magnetically-dilute' P/L of 1/4600 as the subtractant species (Fig. 9; Ref. 4). For each probe concentration below 10 μg I(12, 3)/mg protein, the 1/604 curve is right-shifted from the corresponding 1/4600 curve. Although similar values are seen for $P/L > 1/50$, poorer agreement is observed for lower P/L. For P/L between 1/604 and 1/50, the 1/604 curve consistently underestimates I(12, 3) clustering.

The behavior of the 1/604 curve in Fig. 9 is readily interpreted in terms of the known I(12, 3) distribution in erythrocyte ghosts. Fig. 10 is a schematic diagram showing the relative proportion of dilute and clustered probe in erythrocyte lipid, and is based on % clustering determined

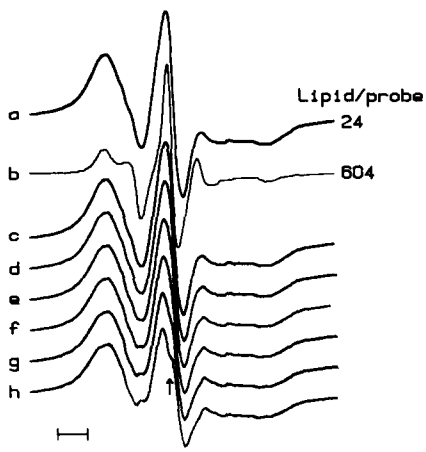

Fig. 7. Subtraction spectra, obtained by subtracting increasing amounts of an intermediate-range spectrum (b) at a $P/L = 1/604$ from another intermediate-range spectrum (a) at a higher loading of $P/L = 1/24$; h_o of (b) is normalized to that of (a). (c) The residual spectrum, with a double-integrated intensity of 99.5% of that of the unsubtracted $P/L = 1/24$ spectrum. (d) This is the spectral endpoint (i.e., 'apparent concentrated' spectrum) of the subtraction as defined in the text. 'Apparent dilute' and 'apparent concentrated' probe are 1 and 99%, and were determined from double integration of the (a) and (d) spectra. (e), (f), (g) and (h) are residual spectra, with double-integrated intensities of 98.5%, 98.0%, 97.5 and 97.0% of that of the unsubtracted $P/L = 1/24$ spectrum. These are oversubtracted, as indicated by the asymmetry of the central band and appearance of a shoulder due to the subtractant spectrum in inverse phase (see arrow). The horizontal bar indicates 10 gauss.

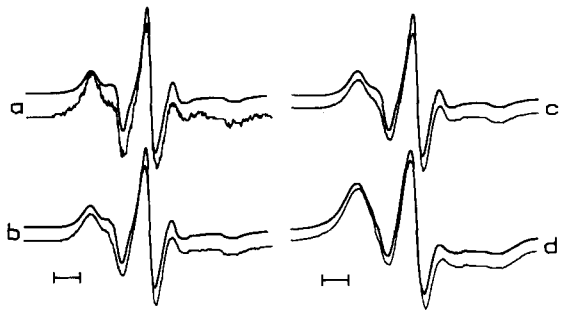

Fig. 8. Intermediate-range spectra and corresponding 'apparent concentrated' spectra, obtained by subtracting out all P/L of 1/604 spectrum from the intermediate spectrum. (a) Top is P/L of 1/303 spectrum (Fig. 4a), while bottom is 'apparent concentrated' component of the 1/303 spectrum (Fig. 4g). (b) Top is P/L of 1/101 spectrum (Fig. 5a), while bottom is 'apparent concentrated' component of the 1/101 spectrum (Fig. 5f). (c) Top is the P/L of 1/75 spectrum (Fig. 6a), while bottom is 'apparent concentrated' component of the 1/75 spectrum (Fig. 6f). (d) Top is the P/L of 1/24 spectrum (Fig. 7a), while bottom is 'apparent concentrated' component of the 1/24 spectrum (Fig. 7d). All h_o are normalized. Horizontal bars indicate 10 gauss.

from the 1/4600 curve in Fig. 9 [4]. It is apparent that 'magnetically-dilute' sites are common to Figs. 10A–D. Furthermore, although 'clustered' probe does not represent a single component, 'concentrated' states appear to be related, with variable-sized clusters being shared to some extent in the various 'concentrated' states. This model was based on an earlier finding that the removal of the 'low' from the intermediate-range spectra does not yield a unique component characteristic of clustered probe, but instead a family of broadened, 'concentrated' spectra with probe-probe interactions ranging from minimal (Fig. 10B, illustrative of Fig. 12b of Ref. 4) to extreme (Fig. 10D, illustrative of the spectrum of Fig. 12e in Ref. 4). Consequently, incremental subtraction of the 1/604 state (Fig. 10B) from either 1/303 (Fig. 10C) or 1/101 (Fig. 10D) would be expected to yield spectral changes observed experimentally with higher loading, since both 'dilute' and 'clustered' states are shared to some extent by all these probe concentrations. Because 'dilute' and 'clustered' states occur in the 1/604 spectrum, however, % 'apparent clustering' for either 1/303 or 1/101 would be expected to be underestimated since subtraction of 1/604 would remove portions

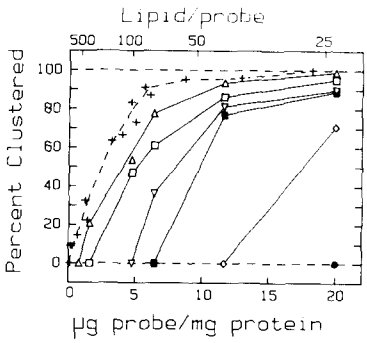

Fig. 9. Plot of the relative percentage of I(12, 3) in 'clustered' states as a function of probe concentration at 37°C. Actual clustered spins (+) were calculated from those present in the concentrated spectrum, obtained at the titration endpoint of subtracting the low-range ($P/L = 1/4600$) spectrum from intermediate-range spectra [4]; 'concentrated' spins were then assessed by double integration of component spectra. 'Apparent clustered' spins were here determined from the residual spectrum, obtained at the titration endpoint of subtracting intermediate-range spectra from spectra at higher loading. Spectra at the following P/L were used as subtractant species: 1/604 (△), 1/303 (□), 1/101 (▽), 1/75 (■), 1/41 (◇) and 1/24 (●). 'Apparent concentrated' spins were assessed by double integration of residual spectra from which all of the subtractant spectrum had been removed (e.g., Figs. 4g, 5f, 6f, 7d). Zero percent 'apparent clustering' for the 1/604, 1/303, 1/101, 1/75, 1/41 and 1/24 curves represents the double integration of the intermediate-range spectrum subtracted from itself (i.e., the null spectrum).

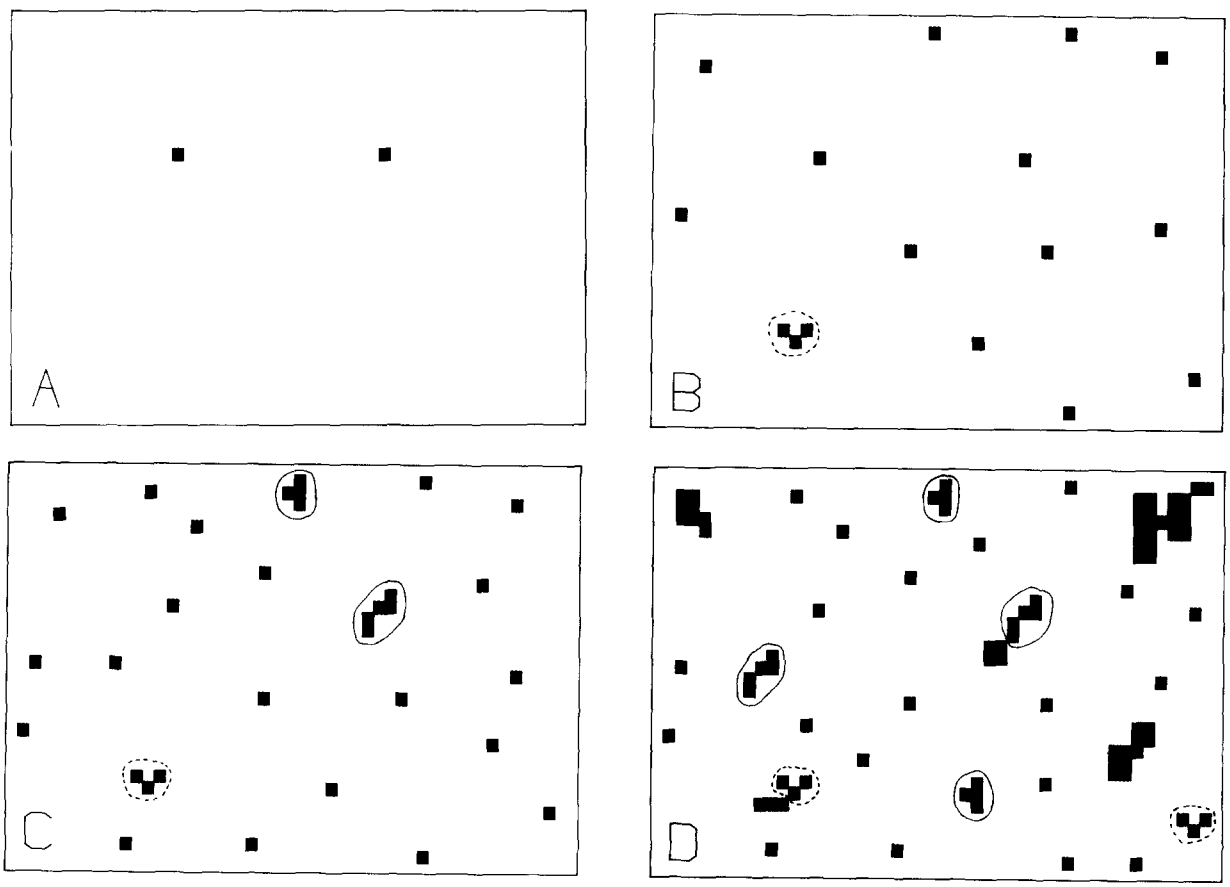

Fig. 10. Schematic of I(12, 3) distribution in human erythrocyte ghosts, calculated from the data of Fig. 9 (+) using a P/L of 1/4600 as the subtractant spectrum, at the following P/L: (A) 1/4600 ('low'); (B) 1/604 ('intermediate'); (C) 1/303 ('intermediate'); and (D) 1/101 ('intermediate'). The diagram is a view perpendicular to the membrane bilayer. For illustrative purposes, the area of I(12, 3) is assumed to be five times that of erythrocyte lipid. Probe molecules are represented by (■), while white space is erythrocyte lipid. % Clustered for lipid/probe ratios of 4600, 604, 303 and 101 are 0, 19, 38 and 78, respectively [4]. Clustered states enclosed by dashed lines are shared in (B), (C) and (D). Similarly, clustered states enclosed by solid lines are shared in (C) and (D).

of all common states. Thus, subtraction of either 1/4600 or 1/604 from higher-range spectra is a meaningful operation due to the nature of the 'dilute' and 'clustered' states occurring in the membrane.

The above suggests that additional % 'apparent clustering' versus probe concentration curves may be constructed, using as the subtractant species P/L of 1/303, 1/101, 1/75 or 1/24. For example, since both 'dilute' and 'clustered' states are common to P/L of 1/303 and 1/101 (illustrated in Fig. 10C, D), subtraction of 1/303 from 1/101 should yield a percent 'apparent clustering' that is less than that obtained with either 1/604 or 1/4600 as the subtractant spectrum (Fig. 9). Indeed, % 'apparent clustering' vs. probe concentration are progressively right-shifted for subtractant spectra with higher probe concentration.

The data in Fig. 9 may be replotted to permit accurate estimation of the probe clustering occurring at a given P/L, even if subtractant spectra free of probe–probe interactions cannot be recorded owing to the technical limitations already discussed in the Introduction. Fig. 11 is a plot of the % (clustering for a spectrum at a given P/L) versus the probe concentration of the subtractant species. Each point is the % 'apparent clustering', obtained from double integration of the residual spectrum left after subtracting to the titration endpoint an intermediate-range spectrum from that of membranes labeled with a higher (or equal) P/L. Each curve in Fig. 11 was constructed from successive subtractions of a given P/L spectrum with spectra measured with a range of P/L. These curves may be extrapolated to a 'zero' probe concentration for the subtractant spectrum (Fig. 11), and the percentage clustering at the y intercept represents the 'best estimate' of the clustering occurring in the original, unsubtracted spectrum. Since no lower P/L than 1/604 was used, the 'best estimate' for the probe clustering at this P/L is zero (Fig. 11).

The above extrapolated % probe clustering values permit a much better estimate of the actual probe clustering than does the 'apparent clustering', assessed by using only the P/L of 1/604 as the subtractant spectrum (Fig. 9). Fig. 12 shows that the 'best estimate' of the probe clustering curve, derived from the extrapolations of Fig. 11,

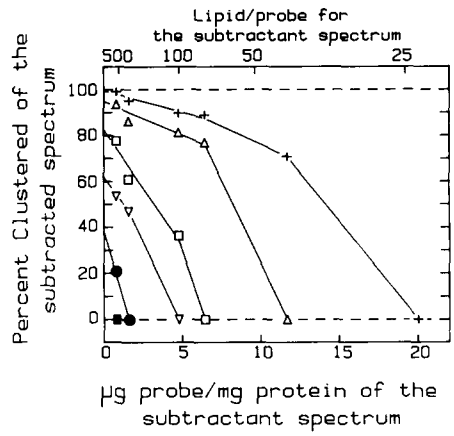

Fig. 11. Plot of the percent probe clustering in the subtracted spectrum versus the probe concentration of the subtractant spectrum. P/L ratios for the subtractant spectra ranged from 1/604 to 1/24. Probe clustering was assessed from the data of Fig. 9. Data points are 'apparent clustering' values which underestimate the actual clustering occurring in the membrane, while extrapolated curves to 'zero' probe concentration represent 'best estimates' of probe clustering (see text). Percent clustering was assigned for membranes labeled with the following P/L: 1/604 (■); 1/303 (●); 1/101 (▽); 1/75 (□); 1/41 (△); and 1/24 (+).

nearly overlap the actual probe clustering values assessed using the 1/4600 spectrum as the subtractant species. It is important to note that the extrapolated % probe clustering in Fig. 12 may be employed to accurately estimate the % clustering in the lowest subtracted spectrum (i.e., P/L of 1/604) used to generate Fig. 11. Without spectra recorded at a lower P/L than 1/604, it is not possible to extrapolate the 1/604 clustering curve to the y intercept of Fig. 11, and the 'best estimate', considering only Fig. 11, would be simply zero (i.e., the double integration of the 1/604 spectrum subtracted from itself). If, on the other hand, 'best estimates' of probe clustering are considered which have been successfully extrapolated to 'zero' probe concentration in Fig. 11, interpolation of Fig. 12 indicates clustering of approx. 19% for a P/L of 1/604. This agrees well with the actual probe clustering observed at this P/L, obtained from earlier spectral subtractions using the 1/4600 spectrum as the subtractant species (Fig. 12; Ref. 4).

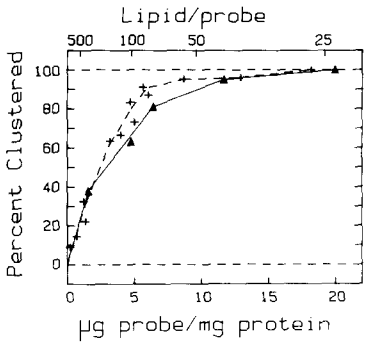

Fig. 12. Plot of actual (+) and 'best estimate' (▲) probe clustering versus probe concentration in human erythrocyte ghosts at 37°C. Actual probe clustering was determined using a 'low' ($P/L = 1/4600$) spectrum as the subtractant species, while 'best estimate' clustering was obtained by extrapolating P/L curves in Fig. 11 to 'zero' probe concentration for the subtractant species. Since no extrapolation was possible for $P/L = 1/604$ in Fig. 11, the 'best estimate' of zero percent for this P/L has been omitted.

Conclusions

Probe–probe interactions occur at extremely low P/L ratios (i.e., 1/2250) in I(12, 3)-labeled human erythrocyte ghosts. For reasons discussed earlier (see above and Ref. 4), the spectral broadening is not accurately described by rapid lateral diffusion of I(12, 3), but is instead due to probe clustering. The spin probe occupies a class of high-affinity, non-interacting sites at low loading. Saturation occurs with increasing probe concentration, and, at higher loading, the probe inserts itself at initially dilute sites to form membrane-bound clusters of variable size. This cluster model readily accounts for the I(12, 3) uptake curve (Fig. 2), if the affinity of occupied sites for I(12, 3) is much less than that of unoccupied sites at low P/L. Low uptake at high P/L may be due either to steric hinderance offered by occupied sites or to high local concentrations of negatively charged probe which repel additional I(12, 3). The validity of the cluster model centers on the accurate simulation of spectral features observed at higher loading by subtracting 'low-range' spectra from 'intermediate-range' spectra. With such subtractions, key spectral parameters (i.e., $2T_{\parallel}$, $2T_{\perp}$. ΔH, and h_{-1}/h_0) change in the direction seen experimentally with increasing P/L. However, it is important to note that such subtractions are unable to generate all of the spectral alterations seen experimentally with increasing probe concentration. Since no single clustered component exists, we are unable to simulate experimental spectra by subtracting a unique 'clustered' component from intermediate spectra. Despite this caveat, the cluster model of Gordon et al. [4] is much more accurate in interpreting the probe uptake and spectral broadening of I(12, 3)-labeled erythrocyte ghosts than previous models.

The new method for estimating probe clustering in human erythrocyte ghosts provides significant advantages over the original protocol set out in Gordon et al. [4]. Even though probe–probe interactions occur for P/L as low as 1/2250 (i.e., 9% 'clustered' probe), Figs. 11 and 12 show excellent estimation of probe clustering over the entire P/L range using only spectra with P/L between 1/604 to 1/24. Indeed, Fig. 11 indicates that a reasonable approximation of the actual probe clustering versus P/L plot in Fig. 12 is possible, even if only spectra between 1/303 to 1/24 are used in extrapolations to the y intercept. Thus, the new iterative subtraction technique permits accurate estimation of probe clustering, without the necessity of recording spectra at extremely low P/L of 1/16000 to 1/4600. This protocol allows for 26- to 53-fold increase in the P/L ratio for the lowest subtractant spectrum, thereby eliminating the need to use high membrane concentrations and signal averaging.

Moreover, this method suggests the P/L range likely to yield 'magnetically-dilute' spectra. 'Best estimates' for probe clustering are first assessed using intermediate-range spectra of 1/604 to 1/24 (Fig. 11), and then plotted over the entire P/L range (Fig. 12). Subsequent interpolation of the 'best estimate' curve with the origin in Fig. 12 permits not only an estimate of the probe clustering in the lowest subtractant spectrum used to generate Fig. 11 (i.e., 19% probe clustering for a P/L of 1/604), but also gives a range of what P/L are likely to yield minimal probe-probe interactions (i.e., at a $P/L < 1/2250$). Both estimates are validated by the actual probe clustering vs. P/L plot in Fig. 12.

The original subtraction technique of Gordon et al. [4] and the iterative subtraction procedure

described here are complementary tools for assigning probe clustering in biological membranes. Under ideal circumstances, the subtraction methodology of Gordon et al. [4] should be used to isolate 'magnetically-dilute' spectra and determine probe clustering. If, however, 'magnetically-dilute' spectra cannot be obtained due to technical difficulties, the iterative subtraction technique is a powerful alternative approach for estimating probe clustering.

Acknowledgments

Dr. L.M. Gordon was a Visiting Scientist of the Division of Chemical and Wood Technology, CSIRO (January–March, 1984). This work was partially supported by grants-in-aid from the American Diabetes Association, Southern California, Inc., the Juvenile Diabetes Foundation, the California Metabolic Research Foundation, the American Heart Association, Orange County and Golden Empire Chapters and National Institutes of Health grant HL/AM-27120.

References

1 Scandella, C.J., Devaux, P. and McConnell, H.M. (1972) Proc. Natl. Acad. Sci. USA 69, 2056–2060
2 Gordon, L.M. and Sauerheber, R.D. (1977) Biochim. Biophys. Acta 466, 34–43
3 Curtain, C.C. and Gordon, L.M. (1984) in Membranes, Detergents and Receptor Solubilization (Venter, J.C. and Harrison, L., eds.), Vol. 1, pp. 177–213, Alan R. Liss, New York
4 Gordon, L.M., Looney, F.D. and Curtain, C.C. (1985) J. Membrane Biol. 84, 81–95
5 Dodge, J.T., Mitchell, C. and Hanahan, D.J. (1963) Arch. Biochem. Biophys. 100, 119–130
6 Hartree, E.F. (1972) Anal. Biochem. 48, 422–427
7 Gaffney, B.J. (1974) Methods Enzymol. 32B, 151–198
8 Gordon, L.M., Sauerheber, R.D. and Esgate, J.A. (1978) J. Supramol. Struct. 9, 299–326
9 Sauerheber, R.D., Gordon, L.M., Crosland, R.D. and Kuwahara, M.D. (1977) J. Membrane Biol. 31, 131–169
10 Gordon, L.M. and Mobley, P.W. (1984) J. Membrane Biol. 79, 75–86
11 Butterfield, D.A., Whisnant, C.C. and Chesnut, D.B. (1976) Biochim. Biophys. Acta 426, 697–702
12 Verma, S.P. and Wallach, D.F.H. (1975) Biochim. Biophys. Acta 382, 73–82
13 Devaux, P., Scandella, C.J. and McConnell, H.M. (1973) J. Magn. Resonance 9, 474–485